^{13}C Solid-State NMR of Gramicidin A in a Lipid Membrane

Per-Ola Quist
Department of Physical Chemistry, Umeå University, S-901 87 Umeå, Sweden

ABSTRACT The natural-abundance ^{13}C NMR spectrum of gramicidin A in a lipid membrane was acquired under magic-angle spinning conditions. With fast sample spinning (15 kHz) at ~65°C the peaks from several of the aliphatic, β-, α-, aromatic, and carbonyl carbons in the peptide could be resolved. The resolution in the ^{13}C spectrum was superior that observed with ^{1}H NMR under similar conditions. The ^{13}C linewidths were in the range 30–100 Hz, except for the α- and β-carbons, the widths of which were ~350 Hz. The β-sheet-like local structure of gramicidin A was observed as an upfield shift of the gramicidin α and carbonyl resonances. Under slow sample spinning (500 Hz), the intensity of the spinning sidebands from ^{13}C in the backbone carbonyls was used to determine the residual chemical shift tensor. As expected, the elements of the residual chemical shift tensor were consistent with the single-stranded, right-handed $\beta^{6.3}$ helix structure proposed for gramicidin A in lipid membranes.

INTRODUCTION

Membrane proteins, residing in lipid bilayers, catalyze vital reactions such as solute transport and charge separation in the living cell (Voet and Voet, 1995). To understand these processes on a molecular scale, knowledge of the structure and orientation of these hydrophobic proteins at high resolution is necessary. The structure of a handful of membrane proteins has been determined by crystallographic methods, although the sample preparation is complicated (Landau and Rosenbusch, 1996). Solid-state NMR has also recently been used to determine the structure of some transmembrane peptides (Griffiths and Griffin, 1993; Opella, 1994).

In a long series of papers, Cross and co-workers have shown that the secondary structure of the transmembrane peptide gramicidin A in oriented lipid bilayers can be determined by solid-state NMR (Cross, 1986; Nicholson and Cross, 1989; Brenneman and Cross, 1990; Teng et al., 1991; Ketchem et al., 1993; Quine et al., 1997). Besides solid-state NMR, geometrical constraints and extensive ^{13}C and ^{15}N labeling were used. A problem in these studies was the necessity for samples with uniformly aligned membranes, which makes the sample preparation difficult and the signal-to-noise ratio low. Recently, new solid-state NMR techniques have been developed to determine the torsion angles in ^{13}C- and ^{15}N-labeled peptides during magic-angle spinning (MAS) of powder samples (Heller et al., 1997; Goetz and Schaefer, 1997; Hong et al., 1997a,b; Feng et al., 1997). It will be interesting to see if these techniques work on peptides in lipid membranes too, where the molecular motion averages the static interactions and the amino acid concentration in the samples is rather low.

If the secondary structure of the peptide is known or the analysis is limited to some few likely structures, the orientation and secondary structure of the peptide in the membrane can be determined by less extensive ^{13}C and ^{15}N solid-state NMR experiments, for instance, by ^{15}N labeling of the amides (Bechinger et al., 1991, 1993, 1996; McDonnell et al., 1993; North et al., 1995) or ^{13}C labeling of the carbonyls in the peptide backbone (Lewis et al., 1985; Cornell et al., 1988; Smith et al., 1989). ^{2}H labeling at various sites has also been used (Hing et al., 1990ab; Prosser et al., 1991; Killian et al., 1992; Ulrich and Watts, 1993), as has ^{14}N NMR (Tycko et al., 1986).

A general drawback of many of these approaches is the need for numerous samples with different combinations of selective labeling in the peptide backbone. This makes the sample preparation complicated and extensive. A solution for this is the new solid-state NMR experiments designed for uniform ^{13}C and ^{15}N labeling (Gross et al., 1995; Wu et al., 1995; Ramamoorthy et al., 1995, 1996; Straus et al., 1996; Baldus and Meier, 1996; Verhoeven et al., 1997; Lesage et al., 1997; Sun et al., 1997; Lambotte et al., 1998).

With all of these techniques in mind, there is an obvious lack of a simple solid-state NMR approach that can be used in the initial studies of a new membrane-bound peptide. That is, a simple approach comprising powder samples, to avoid the difficult orientation on glass plates, that works without ^{13}C or ^{15}N labeling. Yet it should provide information about the peptide orientation in the membrane and suggest a likely secondary structure of the peptide. In this paper we show that this information can be obtained, within ~48 h, from the natural-abundance ^{13}C MAS NMR spectrum from 15–70 mg of a peptide in a lipid membrane. To illustrate the approach, we use the best characterized transmembrane peptide to date, gramicidin A.

The high-speed MAS ^{1}H NMR work on lipid membranes carried out by Oldfield and co-workers about a decade ago was resumed recently (Oldfield et al., 1987; Forbes et al., 1988). Now the focus was on the ^{1}H resonances from gramicidin A and other peptides in lipid membranes (Davis et al., 1995; Bouchard et al., 1995; Le Guernevé and Seigneuret, 1996). In these experiments, the large static line-

Received for publication 22 April 1998 and in final form 27 July 1998.
Address reprint requests to Dr. Per-Ola Quist, Physical Chemistry, Umeå University, S-901 87, Umeå, Sweden. Tel.: 46-90-786-59-73; Fax: 46-90-786-77-79; E-mail: per-ola.quist@chem.umu.se.

0006-3495/98/11/2478/11 $2.00

width caused by the residual ^1H-^1H dipole interactions is reduced by high-speed MAS solid-state NMR. The rapid sample spinning averages out the major part of the dipole interactions and yields linewidths on the order of 50–100 Hz in the ^1H spectrum if the sample spinning is sufficiently fast (Davis et al., 1995).

These works have inspired us to investigate gramicidin A in a lipid membrane with high-speed MAS ^1H and ^{13}C NMR. The aim was to investigate whether the resolution in the ^1H spectrum could be improved and if any interesting information could be derived from the natural-abundance ^{13}C MAS NMR spectrum from gramicidin A. With this in mind, we used a bilayer membrane composed of the zwitterionic surfactant DDAO (*N,N*-dimethyldodecylamine oxide). The major advantage of DDAO is the lack of resonances in the interesting regimes where one usually observes the peaks from the α-protons and α-carbons of the peptide. In addition, DDAO contains no carbonyls, so there are no disturbing resonances in the 160–190 ppm range of the ^{13}C NMR spectrum. Naturally, an ether-linked lipid with a deuterated headgroup and glycerol backbone does the same job as DDAO, although it is not a standard chemical.

In this study we use gramicidin D, which is a natural mixture of antibiotic linear polypeptides with 15 hydrophobic amino acids. The major component (~85%) in gramicidin D is gramicidin A, which has the structure HCO-L-Val^1-Gly^2-L-Ala^3-D-Leu^4-L-Ala^5-D-Val^6-L-Val^7-D-Val^8-L-Trp^9-D-Leu^{10}-L-Trp^{11}-D-Leu^{12}-L-Trp^{13}-D-Leu^{14}-L-Trp^{15}-$NHCH_2CH_2OH$ (Killian, 1992). The remaining fraction in gramicidin D consists of gramicidins with Trp^{11} replaced by tyrosine or phenylalanine, or Val^1 replaced by isoleucine (Killian, 1992). In practice, this means that the NMR spectra of gramicidin D are essentially the spectra of gramicidin A, unless a very favorable signal-to-noise ratio and resolution can be obtained.

Gramicidin A can adopt several secondary structures in lipid membranes. The most stable form is a water and ion channel through the membrane (Urry, 1971, 1972; Veatch et al., 1974; Killian, 1992). The channel is formed by linking two monomers at the N-termini in an antiparallel arrangement (Killian, 1992). Each of the monomers in the dimer forms a single-stranded right-handed $\beta^{6.3}$ helix, with the hydrophobic side chains interacting with the lipid membrane (Ketchem et al., 1993). In this β-helix the hydrogen bonding pattern of the backbone is similar to that in parallel β-pleated sheets (Urry, 1971, 1972; Killian, 1992). The length of the dimer is ~26–30 Å, and the diameter of the channel is ~4–5 Å, which is sufficient to allow passage of small monovalent cations and water (Killian, 1992). The orientation of the channel is along the membrane surface normal (Killian, 1992). In ordinary lipid membranes it is usually possible to add substantial amounts of gramicidin D (or A) without phase separation: molar ratios on the order of one gramicidin to about six to eight lipid molecules are commonly prepared (Killian, 1992; Ketchem et al., 1993). Recently it was shown that the lamellar phase in the ternary system DDAO/gramicidin D/water was stable at a molar fraction of gramicidin/DDAO of less than ~1/6 (Orädd et al., 1995). The properties of this lamellar phase were recently investigated by ^2H-NMR and x-ray scattering (Wästerby and Quist, 1998).

MATERIALS AND METHODS

Sample preparation

The experiments were performed on liquid crystalline samples made of four components; the zwitterionic, single-chained surfactant DDAO (98%; Serva Heidelberg, Germany), gramicidin D (Sigma, St. Louis, MO), heavy water (D_2O, 99.9 atom % D; Aldrich, Milwaukee, WI), and ordinary water (Milli-Q filtered). Because DDAO is hygroscopic it was vacuum dried before use. With the vacuum equipment in our laboratory, about one water molecule per DDAO remains after drying (Vikström, personal communication). The other components were used as supplied.

Samples with three different compositions were investigated. For identification of the ^1H and ^{13}C NMR resonances from DDAO, we prepared a bulk sample with 78.2 weight % DDAO and 21.8 weight % heavy water. The components were mixed to a lamellar phase (Orädd et al., 1995) in a Pyrex tube, which was flame sealed. To obtain a homogeneous composition, the sample was centrifuged back and forth on a daily basis for ~2 weeks and allowed to equilibrate for another 3 weeks. The molar ratio of water to DDAO was 3.2 + 1 in this sample (where the + 1 is the water molecule in "dry" DDAO; cf. above).

For the high-speed MAS experiments, a bulk sample with 27.6 weight % DDAO, 29.4 weight % gramicidin D, and 43.0 weight % D_2O was prepared as follows. First, a dry membrane batch was prepared by dissolving DDAO and gramicidin D in a mixture of chloroform and methanol (in proportion 2:1). This was followed by vacuum drying to a dry membrane batch. Second, the lamellar phase was prepared by mixing appropriate amounts of water and the dry membrane in a Pyrex tube, which was flame sealed. The sample was then mixed as described above, which yields a membrane in which the peptide is a mixture of several conformations. To obtain the most stable peptide conformation, the sample was heated to 60°C for 12 h once a week. The combination of repeated heating and the fact that the pure DDAO membrane is slightly thinner than the height of the gramicidin dimer ensures that gramicidin adopts the single-stranded right-handed $\beta^{6.3}$ helix conformation in the membrane (Killian et al., 1988; LoGrasso et al., 1988; Killian, 1992; Orädd et al., 1995). The molar ratios in this sample were 7.3 DDAO/gramicidin D in the membrane and 17.9 + 1 water molecules per DDAO. Because of the amide protons in gramicidin and the water associated with gramicidin and DDAO, some protons will eventually appear in the water.

For the low-speed MAS experiments, a bulk sample with 62.6 weight % DDAO, 18.7 weight % gramicidin D, and 18.7 weight % ordinary water was used. The sample was prepared as described above. The molar ratios in this sample were 26 DDAO/gramicidin D in the membrane and 3.8 + 1 H_2O/DDAO.

In the high-speed MAS experiments, the 4-mm MAS rotors where filled with ~50 mg sample from the bulk. In the low-speed MAS experiments, the 7.5-mm MAS rotors where filled with ~370 mg sample from the bulk. To slow down the water evaporation for some days, the rotors were sealed with a thin layer of Teflon tape between the rotor and the end caps. No signs of evaporation during the NMR experiments could be observed in the MAS ^1H NMR spectrum before and after the experiments.

NMR experiments

The NMR experiments where performed on a multipurpose Chemagnetics Infinity-400 spectrometer, operating at 400.17 MHz for ^1H and 100.7 MHz for ^{13}C, with an 89-mm bore 9.4-T superconducting magnet.

For the high-speed MAS experiments (2–15 kHz) we used a 4-mm Chemagnetics APEX-II MAS probe. For the low-speed MAS work (0.5–2 kHz) a 7.5-mm Chemagnetics APEX MAS probe was used. An automatic

spinning-speed controller kept the spinning frequency constant to within 1–2 Hz, and an airflow temperature controller kept the temperature constant to within 1–2°C.

To obtain a good signal-to-noise ratio in the ^{13}C spectra we used ramped cross-polarization from ^{1}H to ^{13}C, and cw ^{1}H decoupling during the acquisition (Stejskal et al., 1977; Metz et al., 1994; Zhang et al., 1994). The ramp used 64 linearly increasing rf amplitudes and was applied on the ^{1}H channel. Typical parameters for the experiments on the 4-mm MAS probe at 15 kHz were 3.0 μs ^{1}H 90° pulse (B_{1H} = 83 kHz), 1.5 ms contact time (B_{1H} = 54–62 kHz, B_{1C} = 73 kHz), and 1024 data acquired with a 25-kHz spectral width and ^{1}H decoupling (B_{1H} = 62 kHz). The recycle delay was 3 s. A short contact time (1–2 ms) is necessary, because $T_{1\rho}$ is rather short for the protons in gramicidin. For the flexible DDAO with fairly small residual ^{1}H-^{13}C dipole interaction, the short contact time yields a reduced intensity, particularly for ^{13}C in the ω-methyl group in DDAO, which can be used to optimize the amplitudes in the cross-polarization ramp.

The rf levels were reduced during the experiments with the 7.5-mm MAS probe: 4.0 μs ^{1}H 90° pulse (B_{1H} = 62 kHz), 1.5 ms contact time (B_{1H} = 35–43 kHz, B_{1C} = 39 kHz), and 1024 data acquired with a 25 kHz spectral width and ^{1}H decoupling (B_{1H} = 31 kHz). The recycle delay was 3 s. The TOSS experiments (Dixon, 1982) where performed with ramped cross-polarization, as described above, and compensated π-pulses (B_{1C} = 56 kHz).

RESULTS

High-speed ^{1}H NMR spectrum

Fig. 1 shows the ^{1}H NMR spectrum of the lamellar phase with gramicidin D, DDAO, and water at 15 kHz, at ~65°C. With a nonspinning rotor, the ^{1}H NMR spectrum is a ~10-kHz-wide peak (not shown). An interesting problem connected to the spectrum in Fig. 1 is whether the rapid sample rotation induces structural changes due to the increased temperature and pressure in the rotor.

The temperature in the rotor at 15 kHz was determined using the ^{207}Pb shift of lead nitrate under similar experimental conditions (Bielecki and Burum, 1995; Sparrman et al., manuscript submitted for publication). With a nominal temperature of 50°C, the frictional heating increases the temperature by ~15°C to ~65°C, where the sample is still in lamellar phase. The temperature gradient in the rotor was ~5°C, which may broaden the resonances slightly (Maple and Allerhand, 1986). Furthermore, as discussed by Davis, there is no risk of conformational changes due to the increased pressure (Davis et al., 1995). Phase or conformational transitions are thus unlikely. This conclusion is supported by the presence of spinning sidebands when spinning is at 15 kHz (not shown), which tells us that the ^{1}H NMR spectra in Fig. 1 are due to an anisotropic sample, the lamellar phase. In addition, when we reduce the spinning speed, the intensity of the spinning sidebands increases in a continuous fashion, as reported by others (Forbes et al., 1988; Davis et al., 1995; Le Guernevé and Seigneuret, 1996). Another supporting observation is the ^{1}H spectrum acquired immediately after the rotor was stopped from 15 kHz. This spectrum displays the same wide peak as before the rotor was started. This implies that there was no transition to any isotropic phase, which should manifest itself as a narrow peak. This is because macroscopically separated lyotropic phases merge slowly if not stirred.

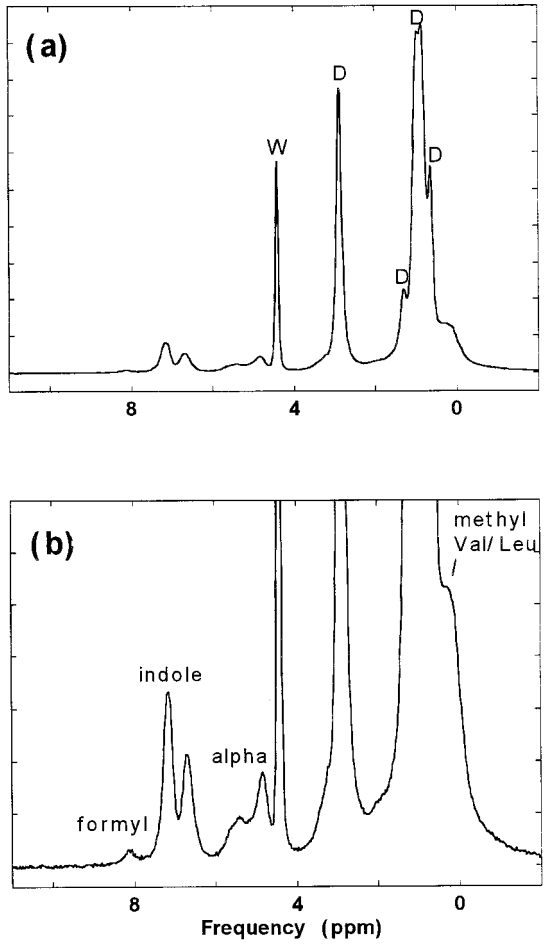

FIGURE 1 The ^{1}H NMR spectrum of a lamellar phase with membranes of DDAO and gramicidin D. The spectrum was recorded at ~65°C and 15-kHz rotor frequency, using a 4-mm MAS rotor. The spectral width was 20 kHz, the number of acquisitions was 32, and the pulse delay was 3 s. In *a* we have identified the peaks from DDAO (D) and water (W). In *b* the vertical scale is expanded four times. The peaks are assigned as discussed in the text. The water peak, which was given the chemical shift 4.4 ppm (Cavanagh et al., 1996), was used as the reference.

By comparison with the corresponding spectrum from a sample with a DDAO/water lamellar phase (not shown), we can identify the peaks from water and DDAO (Fig. 1 *a*). A vertical expansion of Fig. 1 *a* is shown in Fig. 1 *b*, where we observe some peaks from gramicidin A. The water peak at 4.4 ppm was used as an approximate reference (Cavanagh et al., 1996). In the low field region, we observe some peaks at ~8.1, 7.1, and 6.7 ppm, which according to previous studies can be assigned to formyl ^{1}H and the Trp indole ^{1}H (H2-H7), respectively (Veatch et al., 1974; Arseniev et al., 1985; Davis et al., 1995; Le Guernevé and Seigneuret, 1996). Because we use heavy water, the resonances from the backbone amide ^{1}H (~9 ppm) and Trp amide ^{1}H (~10.5 ppm) are difficult to observe in Fig. 1.

The advantage of using DDAO rather than a natural membrane lipid is clearly seen in Fig. 1 *b*, where we observe a wide peak at ~0.3 ppm, which is likely to be the resonances from the γ-protons in Val and the δ-protons in Leu

(Wishart et al., 1991). In addition, we observe two wide peaks at ~4.8 and 5.4 ppm, which should be the resonances from backbone α-protons in gramicidin A (Wishart et al., 1991). The wide peak at ~3.1 ppm (seen as an asymmetry in the base of the leftmost DDAO peak) may be the resonance from some of the β-protons in gramicidin (Wishart et al., 1991). Hence, by using a zwitterionic lipid-like surfactant (rather than a natural membrane lipid), we observe peaks that otherwise are hidden by the intense lipid peaks. Naturally, perdeuterated lipids do the same job, although they are expensive.

The width at half-height of the peaks from gramicidin is ~90–100 Hz, which is similar to the linewidth observed when gramicidin is in dimyristoylphosphatidylcholine (DMPC) or dilauroylphosphatidylcholine membranes (Bouchard et al., 1995; Le Guernevé and Seigneuret, 1996) or in a sample with oriented membranes slowly spinning at the magic angle (Glaubitz and Watts, 1998). It thus appears difficult to reduce the ^{1}H linewidth to the range 10–20 Hz, where NMR experiments like COSY and NOESY are powerful.

High-speed ^{13}C NMR spectrum

Although the resolution in the ^{1}H NMR spectrum is better than one might first expect, it is still not very good. ^{13}C, on the other hand, has a large shift range, and in addition the residual ^{1}H-^{1}H dipole interactions can be removed by proton decoupling. ^{13}C has a better potential for assignment and structure determination than ^{15}N, if the resolution and signal-to-noise ratio are sufficient. This is because ^{13}C has a larger magnetogyric ratio than ^{15}N and there are several connected carbons in the amino acids, but for most of the amino acids there is only one nitrogen.

In Fig. 2 we show the ^{13}C NMR of gramicidin A in a DDAO membrane. The spectrum was obtained with MAS at 15 kHz and ~65°C in a 4-mm rotor. The total number of acquisitions was 20,000 and the pulse delay was 3 s, making a total acquisition time of ~17 h. By comparison with the corresponding spectrum from a sample with a DDAO/water lamellar phase (not shown), we can identify the peaks from DDAO (Fig. 2 *a*). As an internal reference we used the ω-methyl group of the hydrocarbon chain of DDAO, which was given the same chemical shift, 14.0 ppm, as the methyl carbons in *n*-decane (Breitmeier and Voelker, 1987). This choice of reference is, of course, an approximation. However, using the simple empirical expressions derived for ^{13}C shifts in organic solutions (Breitmeier and Voelker, 1987), we can calculate the ^{13}C shift of the γ-ω carbons in DDAO to within 0.2 ppm from the observed shifts. We believe this is because the central part of the membrane resembles an isotropic organic solution. Hence the listed ^{13}C shifts should be correct to within ~±0.2 ppm.

A vertical expansion of Fig. 2 *a* is shown in Fig. 2 *b*, where we observe some fairly narrow peaks from gramicidin A. The resolution is definitely much better than in the corresponding ^{1}H NMR spectrum (Fig. 1 *b*), and there is no problem in identifying peaks from gramicidin in the aliphatic region, the α- and β-carbon regions, the aromatic region, and the carbonyl region (Wishart et al., 1991).

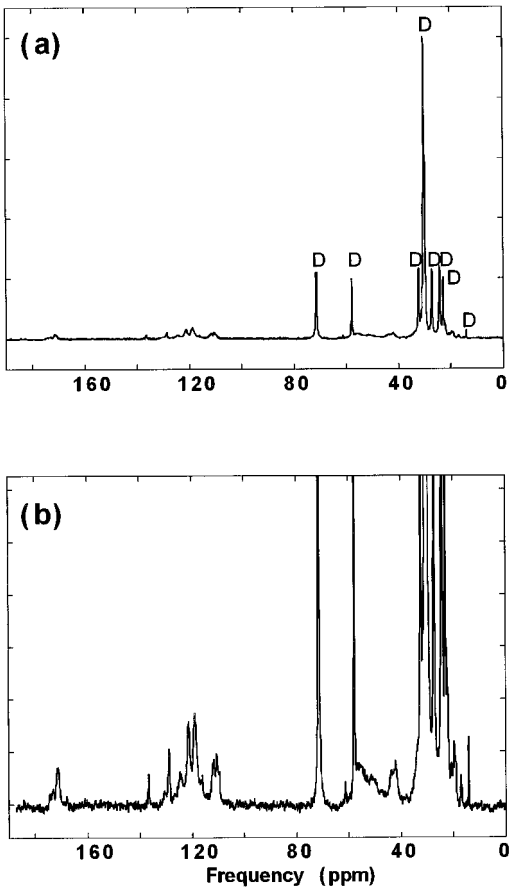

FIGURE 2 The ^{13}C NMR spectrum of gramicidin A and DDAO in a lamellar phase with membranes of DDAO and gramicidin D. The spectrum was recorded at ~65°C and 15-kHz rotor frequency, using a 4-mm MAS rotor. The spectral width was 25 kHz. The spectrum is a sum of two spectra with 10,000 acquisitions each. The total acquisition time was ~17 h. Before Fourier transformation, the FID was multiplied with a 10-Hz exponential window function. In *a* we have identified the peaks from DDAO (D). In *b* the vertical scale is expanded eight times. The peaks are assigned as discussed in the text. The ω-methyl group in the DDAO hydrocarbon chain, which was given the chemical shift 14.0 ppm, was used as the reference.

To clearly display the features in the ^{13}C NMR spectrum we have fitted, with a nonlinear least-squares algorithm, Lorentzian lines to the DDAO and gramicidin peaks in the four regions. The lower traces in Fig. 3, *a*–*c*, is the best fitting ^{13}C lineshape from gramicidin (i.e., the DDAO peaks are not drawn in the lower trace). Fig. 3 *a* shows the spectrum and best fit in the aliphatic region (12–26 ppm), Fig. 3 *b* shows the spectrum and best fit in the α-β region (32–79 ppm), and Fig. 3 *c* shows the spectrum and best fit in the aromatic region (99–144 ppm). The spectral parameters obtained from these fits for the gramicidin peaks are listed in Table 1.

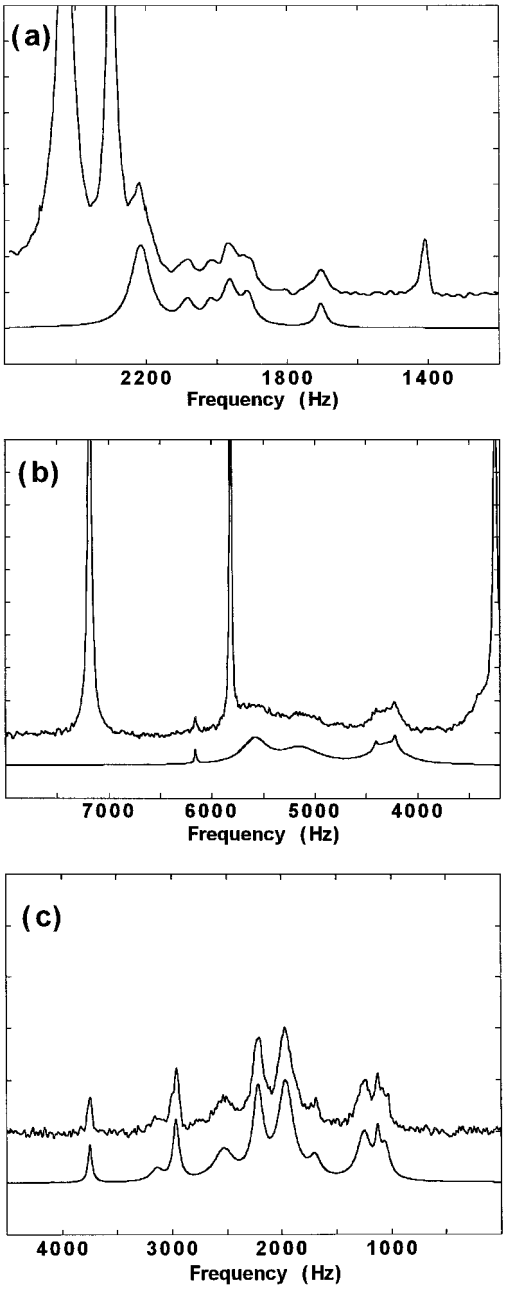

FIGURE 3 Horizontal expansion of the ^{13}C NMR spectrum of gramicidin A and DDAO membranes. (*a*) The aliphatic region. (*b*) The α-β region. (*c*) The aromatic region. The frequency scale is set with respect to the ppm scale in Fig. 2, except in *c*, where the scale is shifted by 10 kHz. Below each spectrum, we display the resulting gramicidin peaks (no peaks from DDAO) from a nonlinear least-squares fit of Lorentzian lines to the ^{13}C resonances from gramicidin and DDAO. Notice that the Hz scale is easily changed to a ppm scale by division with 100 (because the resonance frequency of ^{13}C in this study is 100.7 MHz).

TABLE 1 Parameters derived from a nonlinear least-squares fit of Lorentzian lines to the high-speed MAS ^{13}C NMR spectrum of gramicidin A

Chemical shift* (ppm)	Linewidth# (Hz)	Integral§ (a.u.)	Assignment¶
16.9	32 ± 7	33 ± 5	β-Ala, γ-Val, γ-, δ-Leu
19.0	41 ± 11	49 ± 16	β-Ala, γ-Val, γ-, δ-Leu
19.5	51 ± 13	92 ± 25	β-Ala, γ-Val, γ-, δ-Leu
20.0	37 ± 20	28 ± 17	β-Ala, γ-Val, γ-, δ-Leu
20.7	48 ± 13	46 ± 11	β-Ala, γ-Val, γ-, δ-Leu
22.0	67 ± 4	240 ± 15	β-Ala, γ-Val, γ-, δ-Leu
41.9	40 ± 14	22 ± 6	Ethanol amine?
42.6	360 ± 30	360 ± 20	β-Leu
43.7	42 ± 23	15 ± 6	Ethanol amine?
51.0	450 ± 35	350 ± 20	α-Trp, α-Leu, α-Ala
55.4	285 ± 20	340 ± 20	α-Val
61.2	21 ± 8	14 ± 4	Ethanol amine
109.8	93 ± 20	86 ± 22	Trp-indole
110.5	50 ± 15	50 ± 20	Trp-indole
111.7	150 ± 15	220 ± 20	Trp-indole
116.1	110 ± 30	65 ± 15	Trp-indole
118.8	167 ± 8	490 ± 20	Trp-indole
121.3	112 ± 7	290 ± 15	Trp-indole
124.4	215 ± 25	195 ± 20	Trp-indole
128.7	66 ± 7	120 ± 20	Trp-indole
130.5	120 ± 50	45 ± 15	Trp-indole
136.5	42 ± 7	48 ± 6	Trp-indole
167.7‖	37 ± 2	—	Formyl
171.0‖	93 ± 5	—	Trp carbonyl
171.7‖	95 ± 8	—	Val carbonyl
173.0‖	64 ± 8	—	Leu carbonyl
173.7‖	104 ± 8	—	Ala carbonyl

*Chemical shift is relative to the ω-methyl carbon of DDAO, which was set at 14.0 ppm.
#Assuming one Lorentzian peak. Includes the 10-Hz line broadening applied to the spectra.
§The integrals may differ from the stoichiometric value, because of varying cross-polarization efficiency.
¶See text.
‖Data taken from Table 2.

An interesting feature in Table 1 is the fairly narrow linewidths of many of the gramicidin peaks (which includes the 10-Hz line broadening applied to the spectrum): 30–60 Hz in the aliphatic region, 40–150 Hz in the aromatic region, 40–100 Hz in the carbonyl region (cf. below), and 300–450 Hz in the α-β region. Preliminary ^{13}C MAS NMR results reported by Davis and co-workers give linewidths of ~90 Hz or less for the carbonyl, α-carbon, and methyl carbon resonances from the synthetic peptide $K_2GL_{20}K_2A$-amide in perdeuterated DMPC bilayers (Davis et al., 1995). Similar linewidths were observed for a ^{13}C- and ^{15}N-labeled, α-helical, 15-residue peptide in oriented bicelles (Losonczi and Prestegard, 1998). Those linewidths are comparable to the ones observed here, except for the α-carbon resonances, which are significantly narrower than in gramicidin A. This could be due to a superposition of several slightly shifted, ~100-Hz-wide resonances from the α- and β-carbons in the ^{13}C spectrum from gramicidin. An alternative explanation for the wide α- and β-carbon resonances is slow reorientation of gramicidin in the membrane, which in combination with an effective dipole relaxation from the directly bonded protons yields wide lines (Davis, 1988; Ketchem et al., 1993; Prosser and Davis, 1994). For comparison, the linewidths of the DDAO ^{13}C peaks in Fig. 2 are in the range 20–50 Hz.

Using shift data compiled in the literature (Breitmaier and Voelter, 1987; Wishart et al., 1991; Cavanagh et al., 1996),

we have made a preliminary assignment of the gramicidin peaks in the ^{13}C NMR spectrum (Table 1). A complete assignment is a complicated task, and therefore more experiments must be performed. In general, we expect the resonances from Val, Leu, Trp, and possibly Ala, which are the most abundant residues in gramicidin A.

In the aliphatic region (Fig. 3 *a*), we can distinguish six peaks from gramicidin A. Likely resonances are those from the β-carbon in the Ala residues, the γ-carbons in the Val residues, and the δ-carbons in the Leu residues, which should appear in this region (Cavanagh et al., 1996).

In the α-β region (Fig. 3 *b*), we expect resonances from Val, Leu, Trp, and Ala. Empirical data (Wishart et al., 1991) show that the chemical shifts of the α-carbons of Val, Leu, Trp, and Ala differ by ~5 ppm and increase according to Ala $\approx$ Trp $\approx$ Leu $<$ Val. Hence the peak at 55.4 ppm should be from the α-carbon in the valine residues, and the peak at 51.0 ppm should be the resonances from the α-carbon in the Trp, Leu, and Ala residues. The wide peak at 42.6 ppm is likely from the β-carbon in the Leu residues, which should appear in the region 40–44 ppm (Cavanagh et al., 1996). The resonances from the β-carbons of the other residues are expected in the range 28–35 ppm (Val and Trp) or 16–22 ppm (Ala) (Cavanagh et al., 1996). There are three tiny and narrow peaks at 41.9, 43.7, and 61.2 ppm. We believe that two of these come from the carbons in the ethanolamine group at the C-terminus of gramicidin A, which is less rigid. Hence the linewidth of these peaks should be narrow. The shifts are expected to be similar to those of hydroxyethylamine, which are 44.6 and 64.2 ppm (Breitmaier and Voelker, 1987). We cannot assign the third peak.

In the aromatic region we observe 10 peaks (Fig. 3 *c*), although there are only eight carbons in the Trp indole. However, the Trp indoles are not identically located in the membrane. Rather, they are located at different depths and with different orientations to the membrane normal (Hu et al., 1993; Maruyama and Takeuchi, 1997). Thus it is likely that the resonances from the four Trp indoles are shifted slightly and produce a superposition of peaks. The chemical shift range of the indole resonances (110–135 ppm) observed by us is the same as in organic solutions of gramicidin A (Fossel et al., 1974) and in substituted indoles like gramine (Breitmaier and Voelter, 1987).

In the carbonyl region we observe five peaks (Fig. 4 *a*). Four of these have linewidths of ~60–100 Hz and appear in the range 171.0–173.7 ppm. The fifth peak is less intense and has a linewidth of ~35 Hz and a chemical shift of 167.7 ppm. According to the literature (Wishart et al., 1991), the amino acid carbonyl resonances should appear in the range 171–178 ppm and increase by ~0.5–1 ppm in the order Trp $<$ Val $<$ Leu $<$ Ala. On this basis we assign the peak at 173.7 ppm to Ala, that at 173.0 ppm to Leu, that at 171.7 ppm to Val, and that at 171.0 ppm to Trp. This assignment is not without doubt, although it is likely. The relatively narrow peak at 167.7 ppm is most likely the resonance from the formyl group (HCO) at the N-terminus of gramicidin A.

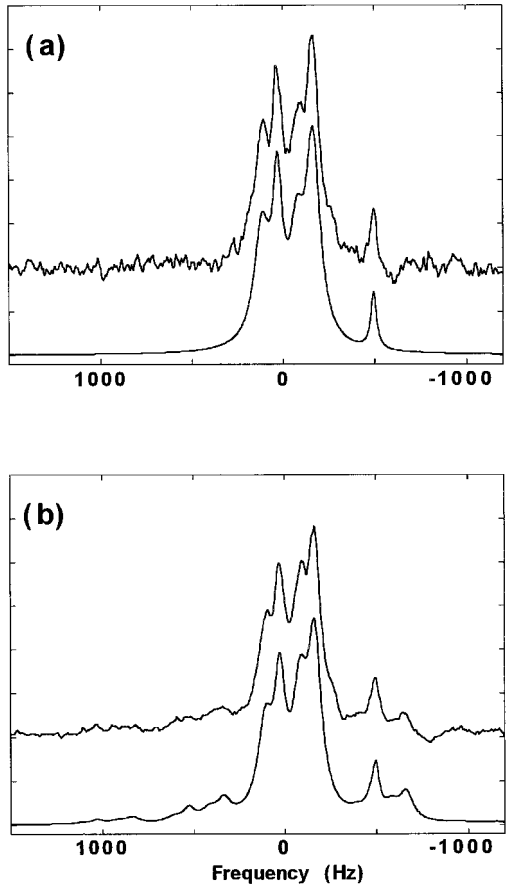

FIGURE 4 The ^{13}C NMR spectrum of gramicidin A in a DDAO membrane. The spectrum has been expanded around the carbonyl region (157–184 ppm). Both spectra where acquired at 50°C, with a spinning speed of 500 Hz. The horizontal scale is in Hz and is shifted by ~17 kHz (cf. Figs. 2 and 3). (*a*) TOSS spectrum, which is a sum of four spectra with 5000 acquisitions each. The total acquisition time was ~17 h. (*b*) Normal cross-polarization spectrum with spinning sidebands, which is a sum of eight spectra with 5000 acquisitions each. The total acquisition time was ~34 h. Below each spectrum, we display the resulting peaks from a nonlinear least-squares fit to the ^{13}C resonances The negative peak at ~−600 Hz (in both panels) is a distortion that was taken care of in the fit, although it is not plotted in the lower trace.

According to the literature (Breitmaier and Voelker, 1987) the chemical shift of the carbonyl in methanoic N-methyl amide is 165.5 ppm (syn) or 168.5 (anti) ppm, which is in the expected range.

The correlation between the protein secondary structure and the isotropic ^{13}C chemical shifts of the α- and carbonyl-carbon resonances (the chemical shift index) can be used as an indication of the secondary structure of peptides in the liquid state (Wishart et al., 1991; Wishart and Sykes, 1994). Because the chemical shift is an essentially local property, we expect the shift of the α- and carbonyl-carbon resonances to be relatively insensitive to the medium outside the peptide, as long as the secondary structure of the peptide does not change. In fact, ab initio calculations have shown that the chemical shift of the α-carbon in a residue is essentially determined by the torsion angles (de Dios et al.,

1993a,b; Heller et al., 1997). Therefore, we also expect this correlation to be valid for membrane-bound peptides. According to the data compiled by Wishart and co-workers, the resonance frequencies of the α- and carbonyl-carbons experience a downfield shift (about +1 to +2 ppm) from the random coil value when in an α-helical conformation, and an upfield shift (about −1 to −2 ppm) when in a β-sheet or extended configuration. Comparison of the α- and carbonyl-carbon chemical shifts in Table 1 with the reference data compiled by Wishart and co-workers shows that these peaks occur at a slightly lower shift (about −1 to −2 ppm) than expected from a random coil. Because ^{13}C shifts are rather temperature insensitive in general (Maple and Allerhand, 1986), the observed shifts indicate a β-sheet-like structure for gramicidin A in the membrane. We believe that this is a significant effect, because the hydrogen bonding pattern and the torsion angles in the single-stranded, right-handed $\beta^{6.3}$ helix of gramicidin are almost identical to those in an ordinary parallel β-pleated sheet (Urry, 1971, 1972; Cross, 1986; Nicholson and Cross, 1989; Brenneman and Cross, 1990, Teng et al., 1991; Killian, 1992; Ketchem et al., 1993; Quine et al., 1997). However, because of the lack of experimental data from membrane peptides, the choice of reference point, and minor temperature effects on the chemical shift, the method should be used with caution until more reference data have been compiled. Yet it is interesting that one can obtain a good indication of the secondary structure from ~15 mg of the unlabeled membrane-bound peptide after only 17 h of acquisition.

Interpretation of spinning sidebands

If the spinning speed is reduced to a level where it is comparable to or less than the anisotropy of the chemical shielding tensor, spinning sidebands, separated by the spinning frequency, will occur around the central peak (Maricq and Waugh, 1979). Analysis of the intensities of the central peak and the spinning sidebands determines the elements of the shift tensor. This has long been done manually (Herzfeld and Berger, 1980), although an iterative fitting routine was published in 1991 (de Groot et al., 1991).

Recently Levitt and co-workers developed a computationally efficient Mathematica program for determination of the chemical shift tensor elements from the intensities of the central peak and the sidebands (Antzutkin, 1996; Antzutkin et al., 1998). We have written a MatLab version of this program. Our code works nicely and fast when tested on the ^{15}N shift tensor of solid ^{15}N-glycine: from a nonlinear least-squares fit of the lineshape for a general shift tensor (Schmidt-Rohr and Spiess, 1994) to the static lineshape of solid ^{15}N-labeled glycine, we determined the elements of the shift tensor. Then, by spinning the sample at some relevant frequencies, we obtained ^{15}N spectra with spinning sidebands. A nonlinear least-squares fit of Levitt's derived lineshape for the spinning sidebands to these spectra converges at the same tensor elements as those determined from the static lineshape. Typically, a spectrum with six spinning sidebands and a central peak is calculated in ~1 s on a 250-MHz Power Macintosh.

In Fig. 4 we show the MAS ^{13}C spectrum of the carbonyl region of gramicidin A in the DDAO membrane. Fig. 4 *a* shows the spectrum from a TOSS experiment at 500 Hz spinning speed. Fig. 4 *b* shows the spectrum obtained from an ordinary ramped cross-polarization experiment. Comparison of these two spectra reveals the spinning sidebands. As the spinning speed is increased to 2 kHz, the spinning sidebands in Fig. 4 *b* disappear (not shown). In Fig. 4 *a* the lower trace shows the best fit of five Lorentzian lines to the TOSS spectrum. The final parameters are listed in Table 2. Notice the fairly narrow lines (60–100 Hz).

Notice that there are no traces of the ^{13}C-^{14}N dipole interaction between ^{14}N and ^{13}C in the carbonyl (Fig. 4 *a*) or the α position (Fig. 3 *b*) in the backbone. This is because of the rapid ^{14}N longitudinal relaxation. The longitudinal relaxation time for ^{14}N in the peptide plane can be estimated from the rotational correlation time of gramicidin A in the membrane, $\sim 10^{-7}$ s (Davis, 1988), the quadrupole interaction of ^{14}N in the peptide group, ~3 MHz (Stewart et al., 1987), and the expression for the angular-dependent relaxation of a quadrupolar nucleus residing in a molecule that performs anisotropic rotational diffusion in a lyotropic liquid crystal (Quist et al., 1991). Assuming that we observe the powder average of the anisotropic relaxation, T_{1N} for ^{14}N in the peptide planes of gramicidin should be ~0.8 μs. This can be compared with the static dipole interaction between ^{14}N and ^{13}C in the α position or in the carbonyl group, which is about d_{NC} = 700 Hz and 940 Hz, respectively. Hence the product $2\pi d_{NC} T_{1N} \ll 1$, which means that the rapid ^{14}N relaxation decouples the dipole interac-

TABLE 2 Parameters derived from a nonlinear least-squares fit to the carbonyl region of the low-speed normal and TOSS ^{13}C NMR spectrum of gramicidin A in a DDAO membrane

Chemical shift* (ppm)	Linewidth# (Hz)	Integral§ (a.u.)	$\sigma_{\parallel} - \sigma_{\perp}$¶ (ppm)
167.7	37 ± 3	380 ± 20	TOSS
171.0	93 ± 5	3300 ± 100	TOSS
171.7	95 ± 8	1600 ± 100	TOSS
173.0	64 ± 8	1700 ± 100	TOSS
173.7	104 ± 8	2100 ± 100	TOSS
167.7	41 ± 3	—	~0
171.0	87 ± 5	—	10.9 ± 0.3
171.7	100 ± 8	—	9.6 ± 0.3
173.0	71 ± 8	—	10.7 ± 0.3
173.7	102 ± 8	—	7.9 ± 0.3

See the text for details.

*Chemical shift is relative to the ω-methyl carbon of DDAO, which was set at 14.0 ppm.

#Assuming one Lorentzian peak. Includes the 10-Hz line broadening applied to the spectra.

§The relative integral may differ from the stoichiometric value, because of varying cross-polarization efficiency. The integral cannot be compared to those in Table 1, because of different experimental conditions.

¶$\sigma_{\parallel} - \sigma_{\perp} = (3/2)\sigma_Z$, where σ_Z is the shift anisotropy of the residual, symmetrical shift tensor of the carbonyl carbon.

tion. This conclusion is also supported by similar observations of other systems (Lewis et al., 1985).

In Fig. 4 *b* the lower trace shows the best fit of Levitt's derived lineshape for the spinning sidebands to the signals in the carbonyl region. Five individual transitions, each having its separate width of the residual shift tensor ($\sigma_{\parallel} - \sigma_{\perp}$), isotropic shift ($\sigma_{iso}$), linewidth (Lorentzian), and intensity were fitted to the spectrum. We thus assume that each resolved peak has an individual residual shift tensor. Because the resolved peaks are superpositions (from several residues of a particular kind), this is a good approximation because of the rigid repeating structure of the peptide, which makes the residual shift tensors of the individual carbonyl resonances similar. Because it is known that gramicidin is diffusing rapidly around the membrane normal and has its aqueous channel along this direction (cf. above), the residual shift tensor should be symmetrical. Consequently, the anisotropy parameter was set to zero during the fit, which helps to determine shift tensor elements (Olivieri, 1996; Hodgkinson, 1997). In this fit, the relative intensities, linewidths, and isotropic shifts converged to the same values as those derived from the TOSS spectrum (Table 2). In addition, for each of the peaks we obtained the width of the residual shift tensor, which was in the range 8–11 ppm (Table 2). As expected, this is less than the principal values of the static chemical shift tensor, $\sigma_{11} - \sigma_{iso} = -74 \pm 3$ ppm, $\sigma_{22} - \sigma_{iso} = -7 \pm 3$ ppm, and $\sigma_{33} - \sigma_{iso} = 82 \pm 3$ ppm (Smith et al., 1989).

Our results can be compared with the studies made by Cornell and co-workers a decade ago (Cornell et al., 1988; Smith et al., 1989), where the width of the residual shift tensor was determined to the range $\sigma_{\parallel} - \sigma_{\perp} = 9$–16 ppm, depending on the amino acid residue under study. As concluded by Cornell and co-workers, this width of the residual shift tensor indicates that the carbonyl bonds are oriented almost parallel to the membrane normal, which is consistent with a rotationally diffusing single-strand $\beta^{6.3}$ helix that is oriented along the membrane normal. On comparison with other likely secondary structures, it turns out that it is only a single-strand $\beta^{6.3}$ helix oriented along the membrane normal that reduces the shift tensor to a width of ~10–15 ppm (depending on the somewhat uncertain orientation of the principal axis system of the shift tensor in the peptide plane) (Lewis et al., 1985; Cornell et al., 1988). For comparison, an α-helix oriented along the membrane normal would reduce the static carbonyl shift tensor to a width of $\sigma_{\parallel} - \sigma_{\perp} \approx 30$ ppm, and a β-pleated sheet structure along the membrane normal reduces the shift tensor to a width of $\sigma_{\parallel} - \sigma_{\perp} \approx 50$ ppm (Lewis et al., 1985). Hence, if we reduce the structure analysis from the general case to a limited number of likely secondary structures, it is indeed possible to determine the peptide structure and orientation from the intensities of the ^{13}C carbonyl spinning sidebands. Notice that this information can be derived from the ^{13}C spectrum of ~70 mg unlabeled peptide in ~34 h. Naturally, we can use the isotropic chemical shifts (from the central peak) of the α- and carbonyl-carbons as another guide to a likely secondary structure (cf. above).

For the formyl carbonyl, the width of the shift tensor is about zero. Together with the fairly narrow linewidth, this implies an increased flexibility at the N-terminus.

Notice that Cornell and co-workers used ^{13}C-labeled analogs of gramicidin A (~7.5 mg in each sample) in a DMPC lamellar phase that was oriented on glass plates. In our study, we use the natural-abundance ^{13}C signal from gramicidin (~70 mg) in a powder sample. Because the magnetic field and other parameters are similar, one expects a much weaker signal from our experiment. However, the linewidth in our experiment is 5–20 times narrower than those observed by Cornell (400–1900 Hz, depending on sample and orientation). This is due to nonperfect alignment (mosaic spread) of the sample on the glass plates, which could be several degrees in "perfectly aligned samples" (Moll and Cross, 1990). Typical ^{15}N linewidths from labeled peptides in membranes aligned on glass plates are also ~1 kHz (Nicholson and Cross, 1989).

From the width of the amino acid carbonyl peaks, we can estimate the correlation time (τ_C) that causes the transverse relaxation of these peaks. Because the proton closest to the carbonyl carbon is ~2.2 Å away (Arseniev et al., 1986; Ketchem et al., 1993), the dominant relaxation mechanism is the chemical shift anisotropy of the carbonyl shift tensor (Abragam, 1978). This means that we can estimate the correlation time from the linewidth at half-height, $\Delta\nu_{1/2} = 1/(\pi T_2)$. With an anisotropic rotational diffusive motion of gramicidin around its aqueous channel (which is along the membrane normal), gramicidin essentially diffuses around the σ_{22} element of the static carbonyl shift tensors, and therefore $1/T_2 = (4\pi^2/15) \cdot (\sigma_{33} - \sigma_{11})^2 \cdot (\nu_0)^2 \cdot \tau_C$ (Suwelack et al., 1980). With a linewidth in the range of 50–100 Hz, a resonance frequency of 100.7 MHz, and $\sigma_{33} - \sigma_{11} \approx 156$ ppm, we obtain a correlation time in the range of $2\text{–}5 \times 10^{-7}$ s. This can be compared with the single correlation time of $\sim 10^{-7}$ s derived from a ^2H relaxation experiment under similar theoretical assumptions, i.e., only one stochastic motional mode (Davis, 1988). Recently it was shown, with ^2H NMR, that the reorientation of gramicidin A in the membrane must be described by (at least) two dynamic modes (Prosser and Davis, 1994): diffusion of the peptide around the membrane normal ($\tau_{R,long} \approx 7$ ns) and diffusive wobbling of this symmetry axis with respect to the membrane normal ($\tau_{R,wobb} \approx 6$ μs), with a rms amplitude of ~16°. (The uncertainty in $\tau_{R,wobb}$ is substantial because the relaxation experiments used probe dynamics on the nanosecond time scale.) Like the anisotropic rotational diffusion, the wobbling motion continues to average the static tensors to a new residual value. The wobbling amplitude of 16° reduces the tensors by ~5% (Kinosita et al., 1977), that is, hardly significantly. Hence the residual NMR tensors observed are essentially due to the anisotropic rotational diffusion of the peptide in the membrane.

The rotational diffusion of gramicidin is thus in the fast limit with respect to the static shift tensor, $(\sigma_{33} - \sigma_{11})2\pi\nu_0\tau_C \ll 1$, whence we observe the residual shift tensor (Abragam, 1978). If, on the other hand, the motion were in the slow limit, the analysis of the intensities of the spinning sidebands would return the static shift tensor. The static shift tensor of the α-carbons can then be used to determine the secondary structure (Heller et al., 1997). In the intermediate regime, where $(\sigma_{33} - \sigma_{11})2\pi\nu_0\tau_C \approx 1$, the motion efficiently broadens the resonances by an exchange mechanism that is isomorphous with relaxation in the Liouville–von Neuman equation (Lynden-Bell, 1971; Ernst et al, 1994). Hence no spinning sidebands can be observed whatever the spinning rate. It is then necessary to change experimental conditions (e.g., the temperature).

DISCUSSION

We have shown that by natural-abundance ^{13}C MAS NMR of membrane-bound peptides it is possible to determine spectral parameters that reflect the peptide orientation, structure, and reorientation in the membrane. With ~15 mg of unlabeled peptide and 17 h of acquisition, we obtain a good indication of the secondary structure. This information is derived from the correlation of the isotropic ^{13}C chemical shift of the α- and carbonyl-carbons with the secondary structure, which has been derived from numerous studies of globular peptides and proteins. With 70 mg of unlabeled peptide and 34 h of acquisition, the secondary structure and the orientation of the peptide in the membrane can be determined from an analysis of the spinning sidebands in the carbonyl region. Although the latter experiment does not determine the orientation and structure unambiguously, it works if we limit the analysis to a selected number of likely secondary structures. It was also possible to make a preliminary assignment of some of the ^{13}C resonances from gramicidin A.

We have also shown that the zwitterionic surfactant DDAO improves the resolution in the ^1H and ^{13}C NMR spectrum. This is mainly because the ^1H and ^{13}C spectra of DDAO have few resonances in the important spectral regions.

In addition, we have shown that the ^{13}C MAS NMR of membrane-bound peptides has a much better resolution than the corresponding ^1H NMR spectrum. Although the intensity is worse, a random ^{13}C labeling of ~10% would produce a ^{13}C MAS NMR spectrum with a signal-to-noise ratio that is ~10 times the signal-to-noise in Fig. 2, with the same acquisition time. Or, put in another way, it has the same signal-to-noise ratio after 10 min of acquisition. Uniform ^{13}C labeling of the peptides may, of course, be a very powerful technique under high-speed MAS conditions, because the residual dipole interactions are averaged out by fast sample spinning and ^1H decoupling. If it is possible to reduce the linewidth of the peptide carbons by a factor of 2–5 (Davis et al., 1995), the $^1J_{CC}$ scalar couplings can be resolved and used to assign the ^{13}C spectrum with standard ^{13}C liquid NMR experiments (Breitmaier and Voelter, 1987; Cavanagh et al., 1996; Lesage et al., 1997) or with the recently developed CP/MAS experiments designed for solid-state NMR work on uniformly labeled samples (Gross et al., 1995; Baldus and Meier, 1996; Straus et al., 1996; Bardet et al., 1997; Verhoeven et al., 1997; Sun et al., 1997; Lambotte et al., 1998).

I am grateful to Prof. Göran Lindblom for comments on the manuscript.

The Swedish Natural Science Research Council (NFR) supported this work. Knut and Alice Wallenbergs Stiftelse is acknowledged for funding the NMR spectrometer used in this work.

REFERENCES

Abragam, A. 1978. The Principles of Nuclear Magnetism. Oxford University Press, Oxford.

Antzutkin, O. N. 1996. Sideband manipulation in magic-angle-spinning nuclear magnetic resonance. Thesis, Stockholm University, Sweden.

Antzutkin, O. N, Y. K. Lee, and M. H. Levitt. 1998. ^{13}C and ^{15}N chemical shift anisotropy of ampillicin and penicillin-V studied by 2D-PASS and CP/MASS NMR. *J. Magn. Reson.* (in press).

Arseniev, A. S., I. L. Barsukov, V. F. Bystrov, A. L. Lomize, and Y. A. Ovchinnikov. 1985. ^1H-NMR study of gramicidin A transmembrane ion channel. Head-to-head right-handed, single stranded helices. *FEBS Lett.* 186:168–174.

Arseniev, A. S., A. L. Lomize, I. L. Barsukov, and V. F. Bystrov. 1986. Gramicidin A transmembrane ion-channel. Three dimensional structure reconstruction based on NMR spectroscopy and energy refinement. *Biol. Membr.* 3:1077–1104.

Baldus, M., and B. H. Meier. 1996. Total correlation spectroscopy in the solid state. The use of scalar couplings to determine the through-bond connectivity. *J. Magn. Reson. A.* 121:65–69.

Bardet, M., L. Emsley, and M. Vincendon. 1997. Two-dimensional spin-exchange solid-state NMR studies of ^{13}C-enriched wood. *Solid State NMR.* 8:25–32.

Bechinger, B., L. M. Gierasch, M. Montal, M. Zasloff, and S. J. Opella. 1996. Orientations of helical peptides in membrane bilayers by solid state NMR spectroscopy. *Solid State NMR.* 7:185–191.

Bechinger, B., Y. Kim, L. E. Chirlian, J. Gesell, J-M. Neumann, M. Montal, J. Tomich, M. Zasloff, and S. J. Opella. 1991. Orientations of amphiphatic helical peptides in membrane bilayers determined by solid-state NMR spectroscopy. *J. Biomol. NMR.* 1:167–173.

Bechinger, B., M. Zasloff, and S. J. Opella. 1993. Structure and orientation of the antibiotic peptide magainin in mebranes by solid-state nuclear magnetic resonance spectroscopy. *Protein Sci.* 2:2077–2084.

Bielecki, A., and D. P. Burum. 1995. Temperature dependence of 207Pb MAS spectra of solid lead nitrate. An accurate, sensitive thermometer for variable-temperature MAS. *J. Magn. Reson. A.* 116:215–220.

Bouchard, M., J. H. Davis, and M. Auger. 1995. High-speed magic-angle spinning solid-state ^1H nuclear magnetic resonance study of the conformation of gramicidin A in lipid bilayers. *Biophys. J.* 69:1933–1938.

Breitmaier, E., and W. Voelker. 1987. Carbon-13 NMR Spectroscopy: High-Resolution Methods and Applications in Organic Chemistry and Biochemistry, 3rd Ed. VCH, Weinheim, Germany.

Brenneman, M. T., and T. A. Cross. 1990. A method for the analytic determination of polypeptide structure using solid state nuclear magnetic resonance. The "metric method." *J. Chem. Phys.* 92:1483–1494.

Cavanagh, J., W. J. Fairbrother, A. G. Palmer, and N. J. Skelton. 1996. Protein NMR Spectroscopy: Principles and Practice. Academic Press, San Diego.

Cornell, B. A., F. Separovic, A. J. Baldassi, and R. Smith. 1988. Conformation and orientation of gramicidin A in oriented phospholipid bilayers measured by solid state carbon-13 NMR. *Biophys. J.* 53:67–76.

Cross, T. A. 1986. Solid state nuclear magnetic resonance approach for determining the structure of gramicidin A without model fitting. *Biophys. J.* 49:124–126.

Davis, J. H. 1988. ^{2}H nuclear magnetic resonance of exchange-labeled gramicidin in an oriented lyotropic nematic phase. *Biochemistry.* 27: 428–436.

Davis, J. H., M. Auger, and R. S. Hodges. 1995. High resolution ^{1}H nuclear magnetic resonance of a transmembrane peptide. *Biophys. J.* 69: 1917–1932.

de Dios, A. C., J. G. Pearson, and E. Oldfield. 1993a. Chemical shifts in proteins: an ab initio study of carbon-13 nuclear magnetic resonance chemical shielding in glycine, alanine, and valine residues. *J. Am. Chem. Soc.* 115:9768–9773.

de Dios, A. C., J. G. Pearson, and E. Oldfield. 1993b. Secondary and tertiary structural effects on protein NMR chemical shifts: an ab initio approach. *Science.* 260:1491–1496.

de Groot, H. J. M., S. O. Smith, A. C. Kolbert, J. M. L. Courtin, C. Winkel, J. Lugtenburg, J. Herzfeld, and R. G. Griffin. 1991. Iterative fitting of magic-angle-spinning NMR spectra. *J. Magn. Reson.* 91:30–38.

Dixon, W. T. 1982. Spinning-sideband-free and spinning-sideband-only NMR spectra in spinning samples. *J. Chem. Phys.* 77:1800–1809.

Ernst, R. R., G. Bodenhausen, and A. Wokaun. 1994. Principles of Nuclear Magnetic Resonance in One and Two Dimensions. Clarendon Press, Oxford.

Feng, X., P. J. E. Verdegem, Y. K. Lee, D. Sandström, M. Eden, P. Bovee-Geurts, W. J. de Grip, J. Lugtenburg, H. J. M. de Groot, and M. H. Levitt. 1997. Direct determination of a molecular torsion angle in the membrane protein rhodopsin by solid-state NMR. *J. Am. Chem. Soc.* 119:6853–6857.

Forbes, J., C. Husted, and E. Oldfield. 1988. High-field, high-resolution proton "magic-angle" sample-spinning nuclear magnetic resonance spectroscopic studies of gel and liquid crystalline lipid bilayers and the effects of cholesterol. *J. Am. Chem. Soc.* 110:1059–1065.

Fossel, E. T., W. R. Veatch, Y. A. Ovchinnikov, and E. R. Blout. 1974. A ^{13}C nuclear magnetic resonance study of gramicidin A in monomer and dimer forms. *Biochemistry.* 13:5264–5275.

Glaubitz, C., and A. Watts. 1998. Magic angle-oriented sample spinning (MAOSS): a new approach toward biomembrane studies. *J. Magn. Reson.* 130:305–316.

Goetz, J. M., and J. Schaefer. 1997. Orientational information in solids from REDOR sidebands. *J. Magn. Reson* 129:222–223.

Griffiths, J. M., and R. G. Griffin. 1993. Nuclear magnetic resonance methods for measuring dipolar couplings in rotating solids. *Anal. Chim. Acta.* 283:1081–1101.

Gross, J. D., P. R. Costa, J-P. Dubacq., D. E. Warschawski, P-N. Lirsac, P. F. Devaux, and R. G. Griffin. 1995. Multidimensional NMR in lipid systems. Coherence transfer through J couplings under MAS. *J. Magn. Reson. B.* 106:187–190.

Heller, J., D. D. Laws, M. Tomaselli, D. S. King, D. E. Wemmer, A. Pines, R. H. Havlin, and E. Oldfield. 1997. Determination of dihedral angles in peptides through experimental and theoretical studies of α-carbon chemical shielding tensors. *J. Am. Chem. Soc.* 119:7827–7831.

Herzfeld, J., and A. E. Berger. 1980. Sideband intensities in NMR spectra of samples spinning at the magic angle. *J. Chem. Phys.* 73:6021–6030.

Hing, A. W., S. P. Adams, D. F. Silbert, and R. E. Norberg. 1990a. Deuterium NMR of Val^{1}-(2-^{2}H)Ala^{3}-gramicidin A in oriented DMPC bilayers. *Biochemistry.* 29:4144–4156.

Hing, A. W., S. P. Adams, D. F. Silbert, and R. E. Norberg. 1990b. Deuterium NMR of ^{2}HCO-Val^{1}-gramicidin A and ^{2}HCO-Val^{1}-D-Leu^{2}-gramicidin A in oriented DMPC bilayers. *Biochemistry.* 29:4156–4166.

Hodgkinson, P., and L. Emsley. 1997. The reliability of the determination of tensor parameters by solid-state nuclear magnetic resonance. *J. Chem. Phys.* 107:4808–4816.

Hong, M., J. D. Gross, and R. G. Griffin. 1997a. Site-resolved determination of peptide torsion angle ϕ from the relative orientations of backbone N-H and C-H bonds by solid-sate NMR. *J. Phys. Chem. B.* 101: 5869–5874.

Hong, M., J. D. Gross, C. H. Rienstra, R. G. Griffin, K. K. Kumashiro, and K. Schmidt-Rohr. 1997b. Coupling amplification in 2D MAS NMR and its application to torsion angle determination in peptides. *J. Magn. Reson.* 129:85–92.

Hu, W., K-C. Lee, and T. A. Cross. 1993. Tryptophans in membrane proteins: indole ring orientations and functional implications in the gramicidin channel. *Biochemistry.* 32:7035–7047.

Ketchem, R. R., W. Hu, and T. A. Cross. 1993. High-resolution conformation of gramicidin A in a lipid bilayer by solid-state NMR. *Science.* 261:1457–1460.

Killian, J. A. 1992. Gramicidin and gramicidin-lipid interactions. *Biochim. Biophys. Acta.* 1113:391–425.

Killian, J. A., K. U. Prasad, D. Hainz, and D. W. Urry. 1988. The membrane as an environment of minimal interconversion. A circular dichroism study on the solvent dependence of the conformational behaviour of gramicidin in diacylphosphatidylcholine model membranes. *Biochemistry.* 27:4848–4855.

Killian, J. A., M. J. Taylor, and R. E. Koeppe. 1992. Orientation of the valine-1 side chain of the gramicidin transmembrane channel and implications for channel functioning. A ^{2}H NMR study. *Biochemistry.* 31:11283–11290.

Kinosita, K., S. Kawato, and A. Ikegami. 1977. A theory of fluorescence polarization decay in membranes. *Biophys. J.* 20:289–305.

Lambotte, S., P. Jasperse, and B. Bechinger. 1998. Orientational distribution of α-helices in the colicin B and E1 channel domains: a one- and two-dimensional ^{15}N solid-state NMR investigation in uniaxially aligned phospholipid bilayers. *Biochemistry.* 37:16–22.

Landau, E., and J. Rosenbusch. 1996. Lipidic cubic phases: a novel concept for the crystallisation of membrane proteins. *Proc. Natl. Acad. Sci. USA.* 93:14532–14535.

Le Guernevé, C., and M. Seigneuret. 1996. High-resolution mono- and multidimensional magic angle spinning ^{1}H nuclear magnetic resonance of membrane peptides in nondeuterated lipid membranes and H_2O. *Biophys. J.* 71:2633–2644.

Lesage, A., C. Auger, S. Caldarelli, and L. Emsley. 1997. Determination of through-bond carbon-carbon connectivities in solid-state NMR using the INADEQUATE experiment. *J. Am. Chem. Soc.* 119:7867–7868.

Lewis, B. A., G. S. Harbison, J. Herzfeld, and R. G. Griffin. 1985. NMR structural analysis of a membrane protein: bacteriorhodopsin peptide backbone orientation and motion. *Biochemistry.* 24:4671–4679.

LoGrasso, P. V., F. Moll III, and T. A. Cross. 1988. Solvent history dependence of gramicidin A conformations in hydrated lipid bilayers. *Biophys. J.* 54:259–267.

Losonczi, J. A., and J. H. Prestegard. 1998. Nuclear magnetic resonance characterization of the myristolated, N-terminal fragment of ADP-ribosylation factor 1 in a magnetically oriented membrane array. *Biochemistry.* 37:706–716.

Lynden-Bell, R. M. 1971. A density matrix formulation of the theory of magnetic resonance spectra in slowly reorienting systems. *Mol. Phys.* 22:837–851.

Maple, S. R., and A. Allerhand. 1986. Ultra-high-resolution NMR. IV. A simple technique for measurements of sample temperature gradients. *J. Magn. Reson.* 66:168–171.

Maricq, M. M, and J. S. Waugh. 1979. NMR in rotating solids. *J. Chem. Phys.* 70:3300–3316.

Maruyama, T., and H. Takeuchi. 1997. Water accessibility to the tryptophan indole N-H sites of gramicidin A transmembrane channel: detection of positional shifts of tryptophans 11 and 13 along the channel axis upon cation binding. *Biochemistry.* 36:10993–11001.

McDonnell, P. A., K. Shon., Y. Kim, and S. J. Opella. 1993. fd coat protein structure in membrane environments. *J. Mol. Biol.* 233:447–463.

Metz, G., X. Wu, and S. O. Smith. 1994. Ramped-amplitude cross polarization in magic-angle-spinning NMR. *J. Magn. Reson. A.* 110:219–227.

Moll, F., III, and T. A. Cross. 1990. Optimizing and characterizing alignment of oriented lipid bilayers containing gramicidin D. *Biophys. J.* 57:351–362.

Nicholson, L. K., and T. A. Cross. 1989. Gramicidin cation channel: an experimental determination of the right-handed helix-sense and verification of β-type hydrogen bonding. *Biochemistry.* 28:9379–9385.

North, C. L., M. Barrabger-Mathys, and D. S. Cafiso. 1995. Membrane orientation of the N-terminal segment of alamethicin determined by solid state ^{15}N NMR. *Biophys. J.* 69:2392–2397.

Oldfield, E., J. L. Bowers, and J. Forbes. 1987. High-resolution proton and carbon-13 NMR of membranes: why sonicate? *Biochemistry.* 26: 6919–6923.

Olivieri, A. C. 1996. Rigorous statistical analysis of errors in chemical-shift-tensor components obtained from spinning sidebands in solid-state NMR. *J. Magn. Reson. A.* 123:207–210.

Opella, S. J. 1994. Solid-state NMR structural studies of proteins. *Annu. Rev. Phys. Chem.* 45:659–683.

Orädd, G., G. Lindblom, G. Arvidsson, and K. Gunnarsson. 1995. Phase equilibria and molecular packing in the *N,N*-dimethyldodecylamine oxide/gramicidin D/water system studied by ^{2}H-NMR spectroscopy. *Biophys. J.* 68:547–557.

Prosser, R. S., and J. H. Davis. 1994. Dynamics of an integral membrane peptide: a deuterium NMR relaxation study of gramicidin. *Biophys. J.* 66:1429–1440.

Prosser, R. S., J. H. Davis, F. W. Dahlquist, and M. A. Lindorfer. 1991. ^{2}H nuclear magnetic resonance of the gramicidin A backbone in a phospholipid bilayer. *Biochemistry.* 30:4687–4696.

Quine, J. R., M. T. Brenneman, and T. A. Cross. 1997. Protein structural analysis from solid-state NMR-derived orientational constraints. *Biophys. J.* 72:2342–2348.

Quist, P.-O., B. Halle, and I. Furo. 1991. Nuclear spin relaxation in a hexagonal lyotropic liquid crystal. *J. Chem. Phys.* 95:6945–6961.

Ramamoorthy, A., L. M. Gierasch, and S. J. Opella. 1996. Three-dimensional solid-state NMR correlation experiment with ^{1}H homonuclear spin exchange. *J. Magn. Reson. B.* 111:81–84.

Ramamoorthy, A., F. M. Marassi, M. Zasloff, and S. J. Opella. 1995. Three-dimensional solid-state NMR spectroscopy of a peptide oriented in membrane bilayers. *J. Biomol. NMR.* 6:329–334.

Schmidt-Rohr, K., and H. W. Spiess. 1994. Multidimensional Solid-State NMR and Polymers. Academic Press, London.

Smith, R., D. E. Thomas, F. Separarovic, A. R. Atkins, and B. A. Cornell. 1989. Determination of the structure of a membrane-incorporated ion-channel: solid-state nuclear magnetic resonance studies of gramicidin A. *Biophys. J.* 56:307–314.

Stejskal, E. O., J. Schaefer, and J. S. Waugh. 1977. Magic-angle spinning and polarization transfer in proton-enhanced NMR. *J. Magn. Reson.* 28:105–112.

Stewart, P. L., K. G. Valentine, and S. J. Opella. 1987. Structural analysis of solid-state NMR measurements of peptides and proteins. *J. Magn. Reson.* 71:45–61.

Straus, S. K., T. Bremi, and R. R. Ernst. 1996. Resolution enhancement by homonuclear J decoupling in solid-state MAS NMR. *Chem. Phys. Lett.* 262:709–715.

Sun, B-Q., C. M. Rienstra, P. R. Costa, J. R. Williamson, and R. G. Griffin. 1997. 3D ^{15}N-^{13}C-^{13}C chemical shift correlation spectroscopy in rotating solids. *J. Am. Chem. Soc.* 119:8540–8546.

Suwelack, D., W. P. Rothwell, and J. S. Waugh. 1980. Slow molecular motion detected in the NMR spectra of rotating solids. *J. Chem. Phys.* 73:2559–2569.

Teng, Q., L. K. Nicholson, and T. A. Cross. 1991. Experimental determination of torsion angles in the polypeptide backbone of the gramicidin A channel by solid state nuclear magnetic resonance. *J. Mol. Biol.* 218: 607–619.

Tycko, R., P. L. Stewart, and S. J. Opella. 1986. Peptide plane orientations determined by fundamental and overtone ^{14}N NMR. *J. Am. Chem. Soc.* 108:5419–5425.

Ulrich, A. S., and A. Watts. 1993. ^{2}H NMR lineshapes of immobilized uniaxially oriented membrane proteins. *Solid State NMR.* 2:21–36.

Urry, D. W. 1971. The gramicidin A transmembrane channel: a proposed $\pi_{(L,D)}$ helix. *Proc. Natl. Acad. Sci. USA.* 68:672–676.

Urry, D. W. 1972. A molecular theory of ion-conducting channels: a field-dependent transition between conducting and nonconducting conformations. *Proc. Natl. Acad. Sci. USA.* 69:1610–1614.

Veatch, W. R., E. T. Fossel, and E. R. Blout. 1974. The conformations of gramicidin A. *Biochemistry.* 13:5249–5256.

Verhoeven, A., R. Verel, and B. H. Meier. 1997. J cross polarization in magic-angle-spinning NMR. *Chem. Phys. Lett.* 266:465–472.

Voet, D., and J. G. Voet. 1995. Biochemistry, 2nd Ed. J. Wiley and Sons, New York.

Wästerby, P., and P.-O. Quist. 1998. Interactions between membranes crammed with gramicidin. *Langmuir.* 13:3704–3709.

Wishart, D. S., and B. D. Sykes. 1994. The ^{13}C chemical-shift-index: a simple method for the identification of protein secondary structure using ^{13}C chemical-shift data. *J. Biomol. NMR.* 4:171–180.

Wishart, D. S., B. D. Sykes, and F. M. Richards. 1991. Relationship between nuclear magnetic resonance chemical shift and protein secondary structure. *J. Mol. Biol.* 222:311–333.

Wu, C. H., A. Ramamoorthy, L. M. Gierasch, and S. J. Opella. 1995. Simultaneous characterization of the amide ^{1}H chemical shift, ^{1}H-^{15}N dipolar, and ^{15}N chemical shift interaction tensors in a peptide bond by three-dimensional solid-state NMR spectroscopy. *J. Am. Chem. Soc.* 117:6148–6149.

Zhang, S., C. L. Czekaj, and W. T. Ford. 1994. Enhancement of polarisation transfer under high-speed MAS using a quasi-adiabatic cross-polarization sequence. *J. Magn. Reson. A.* 111:87–92.